Ionosphere characterization using GPS P3 method by measuring ionospheric delay in Southeast of Brazil and considering geomagnetic storms

F. K. Yamada[1, 2], L. V. G. Tarelho[2], and M. V. Lima[2]

[1] Industrial Fostering and Coordination Institute – IFI, São José dos Campos, SP, Brazil.

[2] National Institute of Metrology, Standardization, and Industrial Quality – INMETRO, Duque de Caxias, RJ, Brazil.

Corresponding author: Fábio Yamada (yamadafky@fab.mil.br)

Key Points:

- Characterization of the ionosphere behavior for the seasons using time scale UTC(INXE) measurements applying the GPS P3 Method.
- Comparison and validation of the GPS P3 Method with the Ionospheric Map Method using Analysis of Variance (ANOVA) during the seasons.
- Observation of the ionospheric behavior, using GPS P3 method during the geomagnetic storms of April 2023 in southeastern Brazil.

Abstract

Ionospheric refraction introduces significant delay and fading in the electromagnetic signals. This makes the ionosphere the most harmful layer of the Earth's atmosphere to the electromagnetic signals emitted by satellites, impacting the reliability of GNSS services. Depending on the ionization level of the ionosphere plasma and the signal frequency, these errors can vary from a few meters to signal unavailability. The main factors influencing ionosphere plasma's ionization level are the intensity of solar radiation and the Earth's magnetic field. The main parameter to evaluate the behavior of the ionosphere is the Total Electron Content (TEC), existing between the satellite and the terrestrial receiver antenna. By predicting the TEC value, it is possible to predict the effects of ionospheric refraction and develop techniques to increase reliability in services that depend on GNSS. This study spans the four seasons from 2018 to 2023, utilizing measurements of ionospheric delays collected by the UTC(INXE). Daily, seasonal, and annual variations in Vertical TEC (VTEC) values are analyzed. A comparative assessment is made between the VTEC values obtained by the GPS P3 method and the Ionospheric Map method for each season until winter 2023. The Analysis of Variance demonstrated the compatibility and comparability of the two methods. Additionally, this investigation explores changes in the ionosphere behavior at the UTC(INXE) location during the geomagnetic storms caused by the solar explosions on April 21, 2023. The findings provide valuable insights for the ionosphere dynamics and can contribute to developing techniques to improve GNSS services' reliability.

Plain Language Summary

Brazil is in a region with one of the planet's largest ionospheric activities. It is located in the equatorial area, and the presence of the South Atlantic Magnetic Anomaly (SAMA) further contributes to this characteristic. In practice, users are susceptible to more significant errors in service measurements that depend on GNSS. In addition to errors perceived directly by users through smartphones, this type of error can affect a country's critical systems, such as telecommunications, energy distribution, and financial systems. These systems require highly accurate timing to operate safely. With increasing dependence on GNSS services, the study of the behavior of the ionosphere becomes essential to guarantee adequate reliability and safety for society.

1 Introduction

The satellites in GNSS constellations constantly send signals towards Earth, also known as observables. However, several systematic errors may occur, such as synchronization errors between the time scales of the satellite and the receiver and errors related to signal propagation in the Earth's atmosphere (ionosphere and troposphere), among others, which hinder the direct measurement of the distance between the satellite and the user's receiver. Therefore, pseudo distance is usually used to refer to the distance calculated by the measurements.

Ionospheric refraction introduces delays in electromagnetic signal propagation, and this delay depends on the signal frequency and the Total Electron Content (TEC) present in the ionosphere. The lower the signal frequency and the higher the ionospheric TEC (or ionization intensity), the greater the refraction in the wave propagation. Consequently, the measurement error will be more significant, varying from a few units to tens of meters or even the loss of the signal link.

The ionization intensity in the ionosphere is directly related to the influence of the Earth's magnetic field and solar radiation. Because the Earth's magnetic field and solar radiation are not constant, it becomes a great challenge to predict the ionization intensity of the ionosphere and, consequently, the error caused by ionospheric refraction in the GNSS electromagnetic signal. The Earth's magnetic field and solar radiation are not constant due to several factors such as long and short-term solar cycles, Earth's magnetic anomalies and activities, seasons, time of day, location of the receiver antenna, and viewing direction, among others. These are temporal and spatial factors that affect the variation in the ionization intensity in the ionosphere, which can be verified when calculating the TEC. The study of the behavior of the ionosphere, through the determination of the TEC, makes it possible to minimize errors in the measurements of GNSS signals caused by ionospheric refraction.

The Earth's tilt, translation, and rotation movements influence the intensity of solar radiation in each planet region. Thus, we have a variation in solar radiation throughout the day and the year's seasons. This variation tends to cause greater ionospheric refraction during the day and summer and less during the night and winter. The magnetic anomaly in the South American region makes it possible to carry out specific studies regarding the behavior of the ionosphere plasma. This anomaly, known as the South Atlantic Magnetic Anomaly (SAMA), presents a less intense magnetic field about the rest of the Earth and can cause peculiar ionosphere behavior.

According to Komjathy (2003), cited by (Matsuoka & Camargo, 2007), Brazil is located in a region that presents one of the most significant variations in the TEC. In recent decades, the Brazilian geodetic community has carried out several studies on the variation of the TEC, taking into account the impact of the ionosphere on positioning, tracking, and related services that use GPS, according to Camargo (1999), Fonseca Junior (2002), Matsuoka and Camargo (2004), Matsuoka et al. (2004), Dal Poz and Camargo (2006), Matsuoka et al. (2006) and Silva (2006) all cited by (Matsuoka & Camargo, 2007).

Using dual-frequency receivers allows the ionosphere-free combination technique to be applied, making it possible to eliminate up to 90% of the first-order ionospheric delay (ITU-T, 2020). However, dual-frequency receivers are expensive and complex, and most users of GNSS services end up using single-frequency receivers, which are simpler and cheaper. Mathematical models and ionospheric maps are typically used to minimize errors caused by ionospheric refraction. For GPS, the mathematical model developed was that of Klobuchar in the 1980s, which offers around 50 % to 60 % correction of the total effect of the ionosphere (Rocha et al., 2015).

Ionospheric Maps can be obtained from centers contributing to the International GNSS Service (IGS) and services specialized in space weather. Global Ionospheric Maps (GIM) provide VTEC values calculated from a network of dual-frequency receivers (Rocha et al., 2015), typically with a resolution of 5º x 2.5º in longitude and latitude, respectively. Initially, these services had a latency of several days, but now, some services make maps available in almost real-time and with better resolutions.

This work aimed to evaluate the behavior of the ionosphere in the southeast region of Brazil from 09/23/2018 to 09/22/2023, applying the GPS P3 method of time and frequency transfer. Data from the UTC(INXE) station was used. The GPS P3 method was compared and validated by the Ionospheric Maps method, provided by the University of La Plata, a tool known as MAGGIA (Mendoza, 2019). It was also possible to observe and analyze the change in the behavior of the ionosphere due to the geomagnetic storms caused by the solar explosion that occurred on April 21, 2023. This section considers temporal and spatial variations of Brazil's southeastern area to do this. The method GPS P3 and the method of ionospheric maps are presented in Section 2, and results and analysis are contained in Section 3. Finally, the conclusions are presented in Section 4.

1.1 - The Total Electron Content (TEC) in the southeastern region of Brazil

The ionosphere lies about 50 to 1000 km altitude and is composed of electrically charged particles called ions. It has a density capable of altering the propagation of electromagnetic waves (Matsuoka et al., 2006). The TEC represents the number of electrons in the electromagnetic signal's path between the satellite and the terrestrial receiver (Santos, 2020). TEC is measured in units of 10^{16} electrons per m^2, equivalent to 1 TECU (TEC Unit), and is the main parameter of the ionization level of the plasma. Brazil's southeastern region presents a lower magnetic field intensity due to a magnetic anomaly called the South Atlantic Magnetic Anomaly (SAMA). The summer period (December to March), where the intensity of solar radiation is higher than the other periods of the year, associated with SAMA presents a scenario that contributes to a significant error caused by ionospheric refraction.

1.1.1 - South Atlantic Magnetic Anomaly (SAMA)

The Earth is surrounded by a magnetic field that significantly influences the behavior and variation of electron density in the ionosphere. The lines of force in this field control the movements of ionized particles, and any change in the geomagnetic field will cause changes in these movements. In the South American region, a peculiarity caused by an anomaly in the Earth's magnetic field alters the ionosphere's behavior. This anomaly is known as the South Atlantic Magnetic Anomaly (SAMA) because it has a weaker magnetic field and is in the region that covers Latin America and the South Atlantic Ocean.

In SAMA, particles spiral along magnetic field lines at around 100 km altitude while this process occurs at around 600 km altitude for regions in the northern hemisphere at equivalent latitude. Because the magnetic field is weaker, there is an effect like that which occurs in polar regions in which there is a continuous flow of energetic particles precipitating and contributing to the ionization of the ionosphere (Jaskulski et al., 2006).

The UTC(INXE) is located in the district of Xerém, municipality of Duque de Caxias (RJ) (22º S; 45º W), which is considered an ionospheric geographical region of low latitude, but this region presents a high level of electron density (Matsuoka el. al., 2006) similar to an equatorial latitude due to an anomaly. The Earth's magnetic field acts as a shield against electrically charged particles coming from space. Depending on the intensity of these particles, a change in the density of terrestrial electrons occurs. This can affect the ionosphere, impacting the signal links between satellites and terrestrial receivers (Frigo & Hartmann, 2018).

1.2 The influence of solar radiation on the Ionosphere

The effects of the ionosphere on electromagnetic signals vary according to its degree of ionization, which in turn depends on the amount of radiation received from the Sun. Thus, there is a variation in the TEC throughout the day due to the Earth's rotational movement. During the day, mainly between 12 pm and 8 pm, ionization is more intense, and during the night, it is lower due to the lower solar incidence in the atmosphere. There is also a seasonal effect where the periods of the seasons must be considered. Summer has a higher incidence of solar radiation compared to winter. This effect is directly related to the inclination of the sun's rays due to the Earth's translational movement around the Sun.

The Sun, in turn, has activity cycles with an average duration of 11 years. The way to monitor the solar cycle is through the number of sunspots. During the cycle period when solar activity is low, the number of sunspots is minimal, just as the peak of solar activity is when the number of sunspots is maximum (NASA, 2021). The most significant number of sunspots is predicted between January and October 2024, according to a forecast update note for the 25th solar cycle from the NOAA (National Ocean And Atmospheric Administration).

At the peaks of solar cycles, events and phenomena, such as explosions and coronal mass ejections, become more frequent and release quantities of charged particles that reach the Earth that can cause disturbances in the geomagnetic field and consequently modify the plasma existing in the ionosphere. Solar flares are eruptions of electromagnetic radiation ranging from a few minutes to hours. The generated electromagnetic energy travels at the speed of light and can instantly impact the lighted side of the Earth's atmosphere. Typically, solar flares are associated with regions where sunspots are more concentrated and magnetic fields are stronger. Explosions are classified based on their magnitudes. The weakest are class B, followed by classes C, M, and class X. Like the Richter earthquake scale, each letter has an internal scale from 1 to 9; between them, a tenfold increase in energy intensity is represented.

Intense solar flares, class M or X, can cause a phenomenon known as Coronal Mass Ejection (CME). Large amounts of plasma are expelled from the surface of the Sun. If the CME occurs towards Earth, the increase in solar wind speed can cause a geomagnetic storm and affect the Earth's atmosphere. As the Earth's magnetic field directly influences the ionosphere's electron density, geomagnetic storms can cause significant variations in the TEC.

1.3 Universal Time Coordinated (UTC) and the GPS P3 method

Universal Time Coordinated (UTC) is the basis of civil time for most countries. UTC is obtained by combining data from around 450 atomic clocks operated by around eighty laboratories in different countries (Panfilo, 2019). In Brazil, the National Institute of Metrology, Quality, and Technology (INMETRO), the National Observatory (ON), and the University of São Paulo (USP-São Carlos) have time scales that contribute to the elaboration of the UTC, and each one has its respective local representation called UTC(k). The letter k represents an acronym of up to 4 letters identifying where and who performs the scale (Whibberley et al., 2011). In the case of INMETRO, k is represented by INXE, comes from **IN**metro **XE**rém, and the technical requirements are met using a commercial cesium standard model HP5071A.

After processing the data provided by atomic clocks, the Free Atomic Scale (EAL, from the French *Echelle Atomique Libre*) is obtained and corrected by primary and secondary frequency standards of greater accuracy. After correction, the International Atomic Time (TAI) is obtained. To ensure agreement between UTC and the time derived from the Earth's rotation (UT1), TAI is compared with UT1, if the difference is greater than 0.9 seconds, a Leap Second is applied (Levine, 2016).

Every month, BIPM issues a CCTF-K001 UTC key comparison report called Circular T, which presents the time differences between UTC and UTC(k). Thanks to new hardware, data processing, and modeling improvements, the uncertainty of synchronizing time scales has been reduced from a few hundred nanoseconds in the early 1980s to less than one ns (Panfilo & Arias, 2019). The geodetic GNSS receiver, connected to the GNSS antenna, receives the electromagnetic signals, and compares the values of the GNSS time scales with the local time scale. This comparison process generates binary files converted to RINEX and CGGTTS files. These files are standardized by IGS/RTCM and CCTF, respectively. The CGGTTS files must be periodically sent to BIPM to contribute to the realization of the UTC.

1.3.1 CCTF Group on GNSS Time Transfer Standards (CGGTTS)

The CGGTTS file is a widely used standard format for scale analysis and accurate time and frequency transfer using GNSS receivers. It covers several satellite constellations such as GPS, Galileo, Beidou, and Glonass (Riehle et al., 2018). Figure 1 shows part of a CGGTTS file. After the header (highlighted in yellow), there is a table (highlighted in green) containing the columns that provide information on the measurements obtained by each satellite. Measurements are consolidated into 16-minute intervals; on average, 6 to 10 satellites are recorded per interval. The number of satellites observed varies according to the line of sight, location, and system installation. The leading information for analyzing ionospheric delay is in the column MSIO, which provides the measured values.

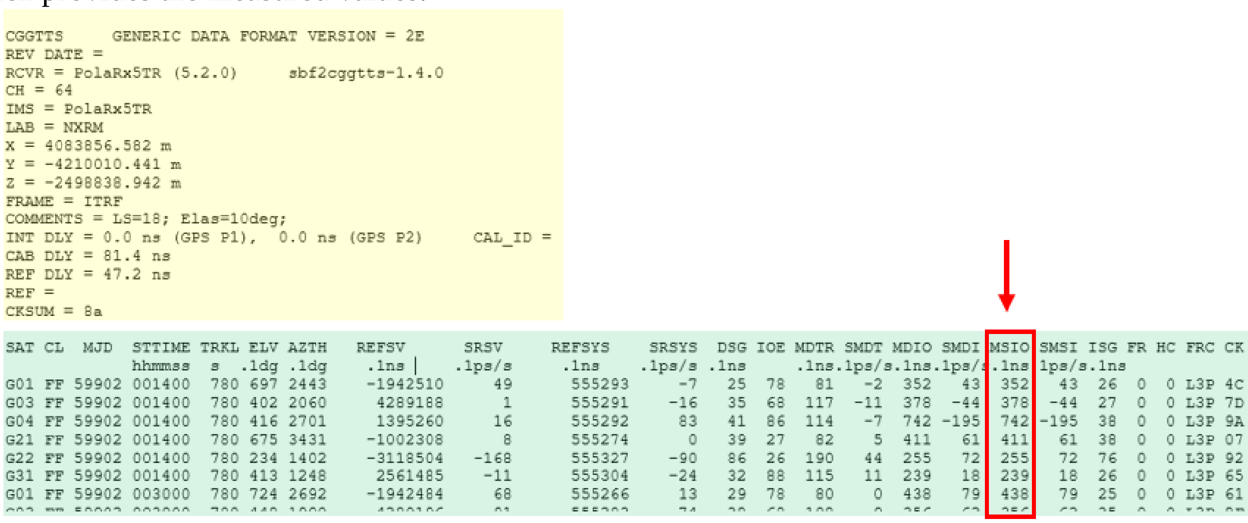

```
CGGTTS     GENERIC DATA FORMAT VERSION = 2E
REV DATE =
RCVR = PolaRx5TR (5.2.0)     sbf2cggtts-1.4.0
CH = 64
IMS = PolaRx5TR
LAB = NXRM
X = 4083856.582 m
Y = -4210010.441 m
Z = -2498838.942 m
FRAME = ITRF
COMMENTS = LS=18; Elas=10deg;
INT DLY = 0.0 ns (GPS P1),  0.0 ns (GPS P2)     CAL_ID =
CAB DLY = 81.4 ns
REF DLY = 47.2 ns
REF =
CKSUM = 8a
```

SAT	CL	MJD	STTIME	TRKL	ELV	AZTH	REFSV	SRSV	REFSYS	SRSYS	DSG	IOE	MDTR	SMDT	MDIO	SMDI	MSIO	SMSI	ISG	FR	HC	FRC	CK
			hhmmss	s	.1dg	.1dg	.1ns	.1ps/s	.1ns	.1ps/s	.1ns		.1ns	.1ps/s	.1ns	.1ps/s	.1ns	1ps/s	.1ns				
G01	FF	59902	001400	780	697	2443	-1942510	49	555293	-7	25	78	81	-2	352	43	352	43	26	0	0	L3P	4C
G03	FF	59902	001400	780	402	2060	4289188	1	555291	-16	35	68	117	-11	378	-44	378	-44	27	0	0	L3P	7D
G04	FF	59902	001400	780	416	2701	1395260	16	555292	83	41	86	114	-7	742	-195	742	-195	38	0	0	L3P	9A
G21	FF	59902	001400	780	675	3431	-1002308	8	555274	0	39	27	82	5	411	61	411	61	38	0	0	L3P	07
G22	FF	59902	001400	780	234	1402	-3118504	-168	555327	-90	86	26	190	44	255	72	255	72	76	0	0	L3P	92
G31	FF	59902	001400	780	413	1248	2561485	-11	555304	-24	32	88	115	11	239	18	239	18	26	0	0	L3P	65
G01	FF	59902	003000	780	724	2692	-1942484	68	555266	13	29	78	80	0	438	79	438	79	25	0	0	L3P	61

Figure 1 – Part of the CGGTTS file (from the author).

The MSIO column provides the inclined ionospheric delay relative to the distance between the receiver antenna and the satellite, measured in the highest value carrier signal. In the case of GPS, it is the L1 signal with a frequency of 1575.42 MHz.

1.3.2 TEC calculation from the CGGTTS files

With the system of the scale UTC properly calibrated, Equation 1.0 calculates the TEC as a function of the ionospheric delay and the signal frequency value (Segantine, 2005).

$$TEC = \frac{v\,c\,f^2}{40.3} \tag{1.0}$$

Where:

TEC = Total Electron Content in electrons / m^2

v = ionospheric delay in seconds;

c = speed of light in meters/seconds;

f = signal frequency in Hz; and

40,3 = constant whose unit is expressed in $\frac{m^3}{s^2 * electrons}$.

1.4 Ionospheric Maps and MAGGIA

Since 1998, the IGS has been providing GIM services with the support of several Ionosphere Associate Analysis Centers (IAAC). GIMs are made available using standardized IONEX (IONosphere map EXchange) files. Ionospheric maps provide Vertical TEC (VTEC) values calculated by collecting measurements from a network of dual-frequency receivers. The main routine, which the IAAC contributes to, involves generating three types of GIM: forecast, rapid, and final. Forecast GIMs are available 1 to 2 days in advance, while rapid and final GIMs are available within 24 hours and 11 days, respectively. With this, it is possible to monitor the TEC through specific tools that make map images with the respective VTEC level available in TECU, online, and free of charge.

The tool developed by the Laboratory of Space Meteorology, Earth Atmosphere, Geodesy, Geodynamics, Instruments and Astrometry (MAGGIA) at the National University of La Plata stands out for the Latin American region. The MAGGIA service is multi-frequency and provides VTEC maps of Latin America and the Caribbean using data from GNSS multi-constellations obtained by more than two hundred ground stations located in several countries in South and Central America, in addition to Africa, Antarctica, and Europe (Mendoza et al., 2019). The tool provides ionospheric maps in almost real-time, as it is updated on the website with a latency of around fifteen minutes.

Ionospheric map services have been an essential tool for studying the behavior of the ionosphere. Its wide space coverage, with short-term availability, has significantly contributed to and assisted in scientific research and industry development to improve services that generally depend on satellite signals.

1.4.1 Single Layer Model (SLM)

Considering that the elevation of the satellites varies depending on their location, the distances between the receiver antenna and the satellites also vary. Consequently, the TEC values will vary proportionally. In this sense, the single-layer ionospheric model (SLM) concept is generally applied in ionosphere modeling research derived from GNSS. SLM considers that all free electrons are concentrated in a layer of infinitesimal thickness. The altitude of this layer varies according to the model adopted by each tool, with values between 350 km and 450 km being common.

The layer's altitude determines the location of the ionospheric point or IPP (Ionospheric Pierce Point), which is the point of intersection in the line of sight between the satellite and the receiver, which passes through this layer. The projection of the IPP on the Earth's surface is called the sub-ionospheric point (Yang et al., 2014). Thus, using the SLM concept, which considers that all electrons are concentrated in the layer, and determining the coordinates of the ionospheric point, it is possible to generate a grid with the TEC values distributed over the layer. One way to apply the SLM is by using the trigonometric function, described according to Equation 1.1 (Dach et al., 2007).

$$F_I\,(z) = \frac{E}{E_v} = \frac{1}{\cos z'} \tag{1.1}$$

Where:

$$sen\, z' = \frac{R}{R+H}\, sen\, z$$

z, z' are the zenith angles at the terrestrial receiver antenna and at the IPP;

R is the radius of the Earth;

H is the height of the simple ionospheric layer about the Earth; and

E and E_v are the TEC values contained in the line of sight (between the satellite and the receiver antenna) and in the vertical projection of the IPP, respectively.

Figure 2 illustrates the SLM where the ionospheric pierce point (intersection in the line of sight between the receiver and the satellite), the sub-ionospheric point (the projection of the ionospheric point on the Earth's surface), the altitude H of the single layer and the angles.

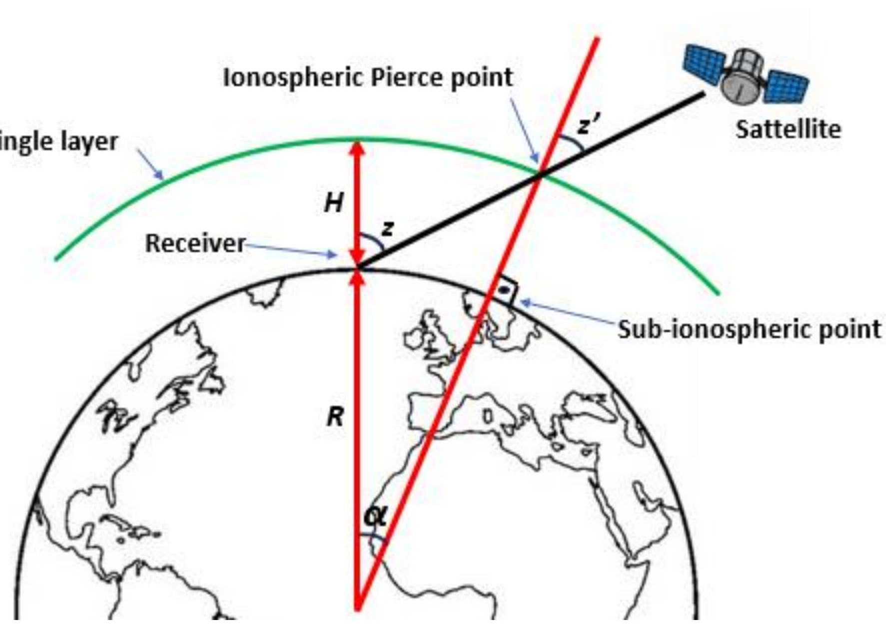

Figure 2 – Single-Layer Model (from author).

According to Matsuoka and Camargo (2004), Skone (2002), and Prol and Camargo (2015), cited by (Prol et. al., 2017), the geographical latitude (ϕ_{ip}) and longitude (λ_{ip}) of the IPP, at a given altitude (h_{ip}), are obtained from the azimuth and elevation angles of the GNSS signal, according to Equations 1.2, 1.3 and 1.4.

$$\phi_{ip} = sen^{-1}[\, sen\, \phi_r \cos\psi + \cos\phi_r\, sen\, \psi \cos Az] \quad (1.2)$$

$$\lambda_{ip} = \lambda_r + sin^{-1}[\frac{sin(\psi)sin(Az)}{\cos(\phi_{ip})}] \quad (1.3)$$

With:

$$\psi = \frac{\pi}{2} - El - sin^{-1}\, [\frac{r_e}{(r_e + h_{ip})} \cos(El)] \quad (1.4)$$

Where:

ϕ_r and λ_r are the latitude and longitude of the terrestrial receiver, in radians;

r_e is the radius of the Earth equal to 6371 km;

Az and El are the azimuth and elevation angles of the GNSS signal, in radians.

h_{ip} is the altitude of the IPP layer (usually 350 km or 450 km).

1.4.2 **ION**osphere Map **EX**change (IONEX) and VTEC calculation

From a workshop held by IGS in 1996, the first step to begin a comparison of TEC maps derived from GPS was done through a standardization proposed by JPL. The significant conclusion was that defining a file format for exchanging, comparing, or combining TEC maps or ionospheric maps was necessary. Thus, the IONEX format emerged, which allows the exchange of two- and three-dimensional maps generated from a geographic reference (Feltens & Schaer, 2015).

Each IONEX file consists of a header section and a data section. The header is mandatory and contains general information such as the IONEX version, program name, date and time the file was generated, brief description of the applied model, start and end of the map (containing date, hour, min and second), function mapping used, elevation cutoff, observables collected, number of stations and satellites as well as GNSS observed, initial and final latitudes and longitudes as well as the step (DLAT and DLON) applied, among other important information for the user. Just below the header, the IONEX data section begins with the period that IONEX covers, containing the year, month, day, hour, minute, and second. Then, a series of VTEC measurement groups begins, which depend on the initial and final latitudes and longitudes.

According to (Feltens; Schaer, 1998), it is possible to use three different types of TEC E processing, depending on the geocentric latitude β, longitude λ and universal time t, when TEC maps $E_i = E(T_i)$, $i = 1, 2, ..., n$ (applying interpolation or using the closest TEC value at a given time). However, when the IONEX grid is dense enough, it is possible to use the simple four-point Equation 1.5.

$$E(\lambda_0 + p\Delta\lambda, \beta_0 + q\Delta\beta) = (1-p)(1-q)E_{0,0} + p(1-q)E_{1,0} + q(1-p)E_{0,1} + p\,q\,E_{1,1} \quad (1.5)$$

Thus, for a given location, it is possible to calculate the VTEC value from the four VTEC values closest to the location of interest.

2 Materials and Methods

The behavior of the ionosphere was characterized by the GPS P3 method for the four seasons between September 2018 and September 2023, totaling five years. The values of the MSIO column's ionospheric delays and the GPS L1 signal frequency made it possible to calculate the TEC. For comparison with the ionospheric map method, applying the SLM at an altitude of 450 km was necessary to obtain the respective VTEC.

An ANOVA was carried out to validate the GPS P3 method between the VTEC values of seasons between September 2022 and September 2023. The calculation of the VTEC values, using the ionospheric map method, considered the exact location coordinates of UTC(INXE) and the dense MAGGIA grid enough to use Equation 1.5.

To characterize the ionosphere relative to the seasons, the VTEC for the 24 hours of each day was initially calculated, and then the average of the days relative to the period of each season. Due to the volume of data, it was necessary to develop a program called VtecGraph3 in Python programming language to process the data.

2.1 VTEC calculation using the GPS P3 method

To enable the comparison and validation with the ionospheric map reference method (IONEX), first, it is necessary to calculate the “vertical” ionospheric delay to obtain the respective VTEC. For this, the concept of SLM, presented in Equation 1.1, is applied, using the ionospheric delay values instead of the TEC, according to Equation 2.0.

$$F_I(z) = \frac{MSIO}{MSIO_v} = \frac{1}{\cos z'} \qquad (2.0)$$

Where :

$\sin z' = \frac{R}{R+H} \sin z$

z, z' are the zenith angles at the terrestrial receiver antenna and at the IPP;

R is the radius of the Earth equal to 6.317 km;

H is the altitude of the single ionospheric layer model about Earth used in MAGGIA (450 km); and

$MSIO$ and $MSIO_v$ are the values of the ionospheric delays in the line of sight (between the satellite and the receiver antenna) and the vertical projection of the IPP, respectively.

Determining the *MSIOv* values makes it possible to calculate the respective VTEC using Equation 2.1 (Equation 1.0 adapted).

$$VTEC = \frac{c\,f^2}{40.3} * MSIO_V \qquad (2.1)$$

Where:

$MSIO_V$ = “vertical” ionospheric delay in seconds;

c is the speed of light equal to 299792458 m / s;

f is the value of the GPS L1 carrier frequency equal to 1,57542 GHz; and

40.3 is the constant whose unit is expressed in $\frac{m^3}{s^2 * electrons}$.

Then, using the elevation, azimuth, and altitude of the single layer, the location coordinates of the sub-ionospheric point of each signal are determined. Considering that the sub-ionospheric points are at the same altitude as the receiver antenna, the distances of each sub-ionospheric point about the receiver antenna are calculated. Thus, for each group of 16 min measurements, the average VTEC weighted by distances is calculated, that is, the closest VTEC having a more significant weight about the VTEC furthest from the receiver.

For example, Figure 3 presents seven measurements (d0 to d6) relative to an interval of 16 min. Each VTEC measurement (Δ) has a distance *d* about the location of the NXRA receiver antenna, with *d0* being the smallest distance and *d6* being the largest distance.

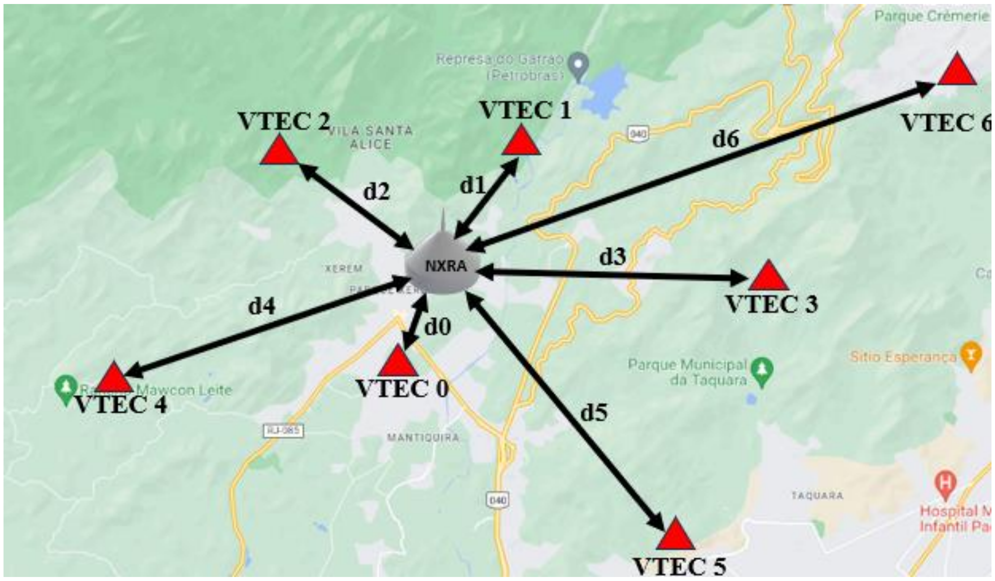

Figure 3 – Example of a group of 16-minute VTEC measurements (from the author).

First, the latitude and longitude of each IPP must be calculated to calculate distances. For this, the geometric method presented in Equations 1.2, 1.3, and 1.4 is applied using the elevation and azimuth of each measurement, available, respectively, in the ELV and AZTH columns of the CGGTTS file. With the coordinates determined, the distances are calculated, and finally, the average value of VTEC measurements is calculated for each 16-minute interval, weighted by distances, according to Equation 2.2. The weight of each measurement is proportional to its distance from the receiver, with the closest measurement having the most significant weight and the most distant measurement having the lowest weight, according to the criteria in Equation 2.3.

$$VTEC_{Méd\ Pond} = \frac{VTEC_0\frac{d0}{d0} + VTEC_1\frac{d0}{d1} + VTEC_2\frac{d0}{d2} + VTEC_3\frac{d0}{d3} + VTEC_4\frac{d0}{d4} + VTEC_5\frac{d0}{d5} + VTEC_6\frac{d0}{d6}}{\frac{d0}{d0}+\frac{d0}{d1}+\frac{d0}{d2}+\frac{d0}{d3}+\frac{d0}{d4}+\frac{d0}{d5}+\frac{d0}{d6}} \quad (2.2)$$

Considering Equation 2.3 being:

$$\frac{d0}{d0} = 1\ e\ \frac{d0}{d0} > \frac{d0}{d1} > \frac{d0}{d2} > \frac{d0}{d3} > \frac{d0}{d4} > \frac{d0}{d5} > \frac{d0}{d6} \quad (2.3)$$

The total measurement uncertainty of the VTEC measured by the GPS P3 method for each 16-minute measurement group is calculated using Equation 2.4.

$$\sigma_{VTEC\ TOTAL} = \sqrt{\sigma^2_{VTEC\ B} + \sigma^2_{VTEC\ A}} \quad (2.4)$$

Where:

$\sigma_{VTEC\ A}$ is the measurement uncertainty of Type A; and

$\sigma_{VTEC\ B}$ is the measurement uncertainty of Type B.

$$\sigma_{VTEC\ A} = \frac{\sqrt{\frac{\sum_{i=1}^{n}(x_i - \overline{x_i})^2}{(n-1)}}}{\sqrt{n}} \quad (2.5)$$

Where x_i is the VTEC measured for each satellite, according to Equation 2.1, $\overline{x_i}$ is the weighted average VTEC (according to Equation 2.2), and n is the number of satellites observed in the respective 16 min interval.

$$\sigma_{VTEC\ B} = \frac{\sqrt{((\frac{\partial \frac{f^2 v}{40,3}}{\partial v})^2 * \sigma_v^2) + ((\frac{\partial \frac{f^2 v}{40,3}}{\partial f})^2 * \sigma_f^2)}}{10^{16}} \quad (2.6)$$

Where:

$\sigma_{VTEC\ B}$ is the aplicattion of “general law of error propagation” (BIPM, 2008) at Equation 1.0;

f is the L1 carrier frequency equal to 1575.42 MHz;

v is the average reference ionospheric delay in meters;

σ_v is the standard deviation of the ionospheric delay in meters;

σ_f is the standard deviation of the L1 frequency (1575,42 MHz) equal to 10 KHz.

2.2 VTEC calculation using the ionospheric maps method

After downloading the IONEX files from the MAGGIA tool repository, the VtecGraph3 program calculates the VTEC by interpolating the four values closest to the location of the NXRA receiver, according to Equation 1.2. Considering that there are 96 measurements per day, an adjustment takes the average of the first two measurements (first and second), the 16th and 17th measurement, the 32nd and 33rd measurements, the 48th and 49th measurements, the 64th and 65th measurements, the 80th and 81st measurements and the last two measurements of the day (95th and 96th). Thus, the same number of measurements as the GPS P3 method are obtained for the ANOVA.

The total measurement uncertainty of VTEC, measured by the ionospheric map method every 15 minutes, is calculated using Equation 2.7.

$$\sigma_E = \sqrt{((\frac{\partial E}{\partial p})^2 * \sigma_p^2) + (\left(\frac{\partial E}{\partial q}\right)^2 * \sigma_q^2\right) + \left(\left(\frac{\partial E}{\partial E}\right)^2 * \sigma_E^2\right)} \quad (2.7)$$

Where:

σ_E is the aplicattion of “general law of error propagation” (BIPM, 2008) at Equation 1.5;

p is the weighting in longitude, equal to 0.4, dimensionless;

σ_p is the standard deviation of the longitude weighting, equal to 0.1, dimensionless;

q is the weighting in latitude, equal to 0.8, dimensionless; and

σ_q is the standard deviation of the weighting in latitude, equal to 0.1, dimensionless;

2.3 Comparison and validation of methods

ANOVA is a statistical technique that makes it possible to assess whether significant differences exist between the means of groups or independent populations. An assessment of the variation within and between the groups involved is conducted. Two hypotheses are defined for the analysis: H_0 or null and H_1 or alternative. The null hypothesis considers that the groups of values analyzed have equal or close population means. In contrast, the alternative hypothesis considers that the population means are different, or at least one means differs from the others.

If $F_{cal} < F_{critical}$, it is considered H_0; otherwise, if F calc > F critical, H_0 is rejected. The significance level adopted will be $\alpha = 5\%$, and considering $k = 2$ and $N = 89$, we have the F critical from the Snedecor F distribution table equal to approximately 3.920 (NIST/SEMATECH, 2012).

2.4 Observation of the geomagnetic storm – April 24, 2023

The British Geological Survey (BGS) is a geoscience research center that belongs to UK Research and Innovation (UKRI) and is affiliated with the Natural Environment Research Council (NERC) (BGS, 2023). Suppose an event detected on the Sun could cause a geomagnetic effect on Earth. In that case, the BGS issues an alert about the event's possible impacts on Earth.

On April 24, 2023, an alert was issued about a CME that had reached Earth at the end of the previous day, causing significant disturbances in the Earth's magnetic field. This CME was associated with a long-lasting M-class solar flare on April 21 at 5:44 pm (Universal Time). High rates of geomagnetic activity were observed by meters located in the United Kingdom and Ireland.

On that occasion, auroras were observed in several points in the northern hemisphere. Considering the events above, the VtecGraph3 Program was used to observe the ionosphere's behavior between April 21st and 25th, 2023, in the location coordinates of the UTC (INXE) time scale. The main objective was to verify whether and how the geomagnetic storm, observed by magnetometers in the United Kingdom and Ireland region, changed the behavior of the ionosphere in Brazil's southeast region, applying the GPS P3 method.

3 Results and analysis

Applying the procedure in section 2.1, using the ionvtec_p3_final.py module from the VtecGraph3 program, the VTEC graphs were obtained for the spring, summer, autumn, and winter seasons, as shown in Figure 4 (Yamada, 2024).

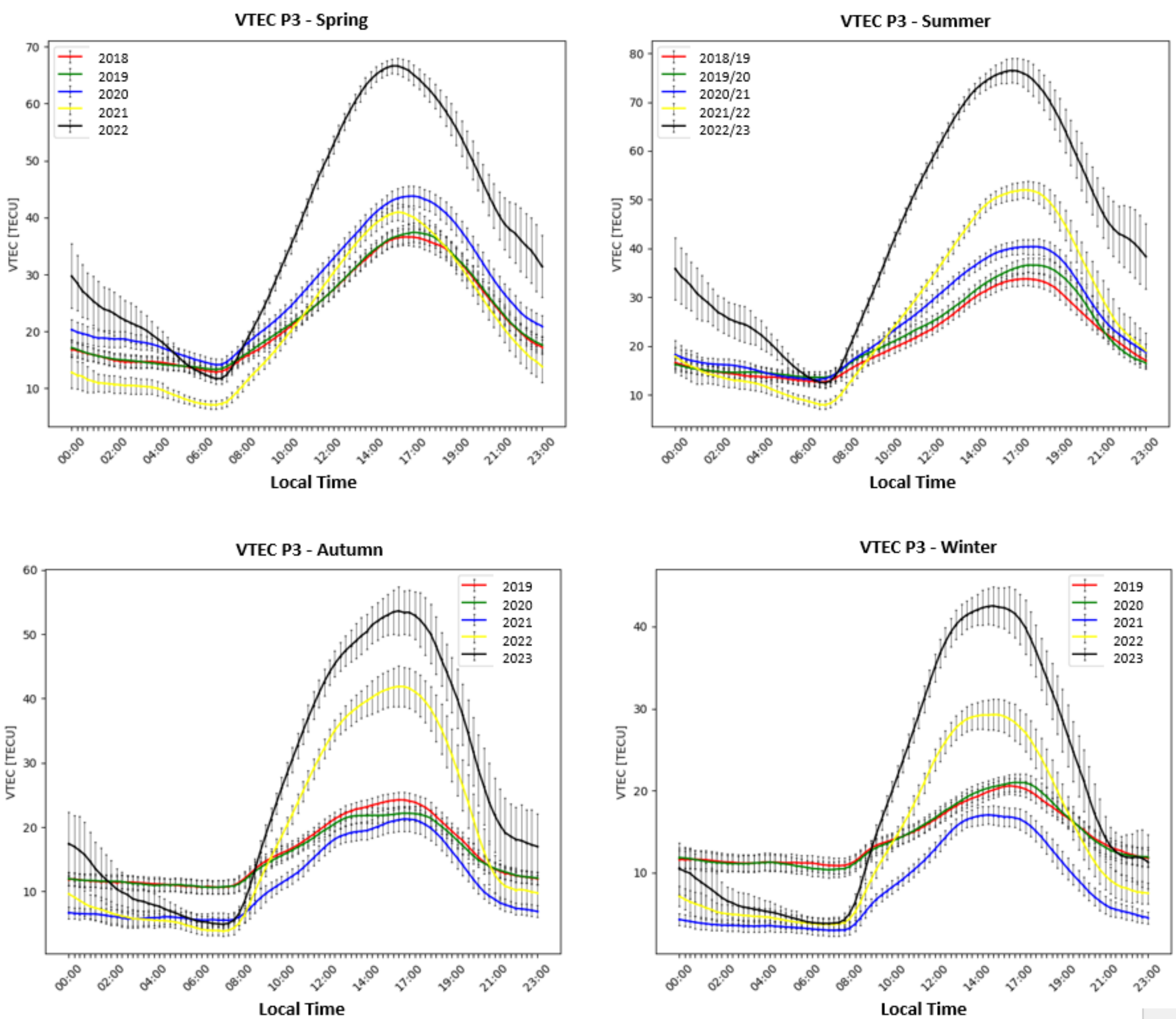

Figure 4 – Characterization of the ionosphere using the GPS P3 method in Southeast Brazil during seasons (from author).

Observing the **hourly variation** of VTEC is possible due to the Earth's rotation movement. At night and in the morning, generally between 0 am and 8 am, the VTEC is lower. From 8 am onwards, with the increase in solar radiation, there is an increase in VTEC, reaching its peak between 4 pm and 5 pm. Then, with the decrease in solar radiation and the beginning of the night period, VTEC decreases.

Seasonal variation is also observed when comparing the behavior of VTEC between seasons for the same year. Due to the Earth's translational movement, summer has the highest incidence of solar radiation, followed by spring, autumn, and winter. For example, for the seasons of 2021 and 2022, the spring (2021) and autumn (2022), considered intermediate seasons, presented VTEC variations between approximately 4 and 40 TECU and 3 and 40 TECU, respectively. Meanwhile, the summer (2021/22) and winter (2022) months presented variations between 5 and 50 TECU and 5 and 28 TECU, respectively.

For each season, annually (starting in 2018), it is also possible to observe an increase in the variation (VTECmax – VTECmin) or the maximum daily value of VTEC. In most cases, both occur, showing an **annual variation.** For example, for the summer of 2018/2019, the daily variation was around 21 TECU (13 to 34 TECU, between 7 am and 6 pm), and for the summer of 2022/2023, this variation was around 62.5 TECU (12.5 to 75 TECU, between 7 am and 6 pm). An increase in daily variation of more than 200 % and more than 150 % in the maximum daily value. The results of the comparison between the two methods, applying the procedure in section 2.2, using the ionvtec_validation.py module from the VtecGraph3 program, are presented in Figure 5 (Yamada, 2024).

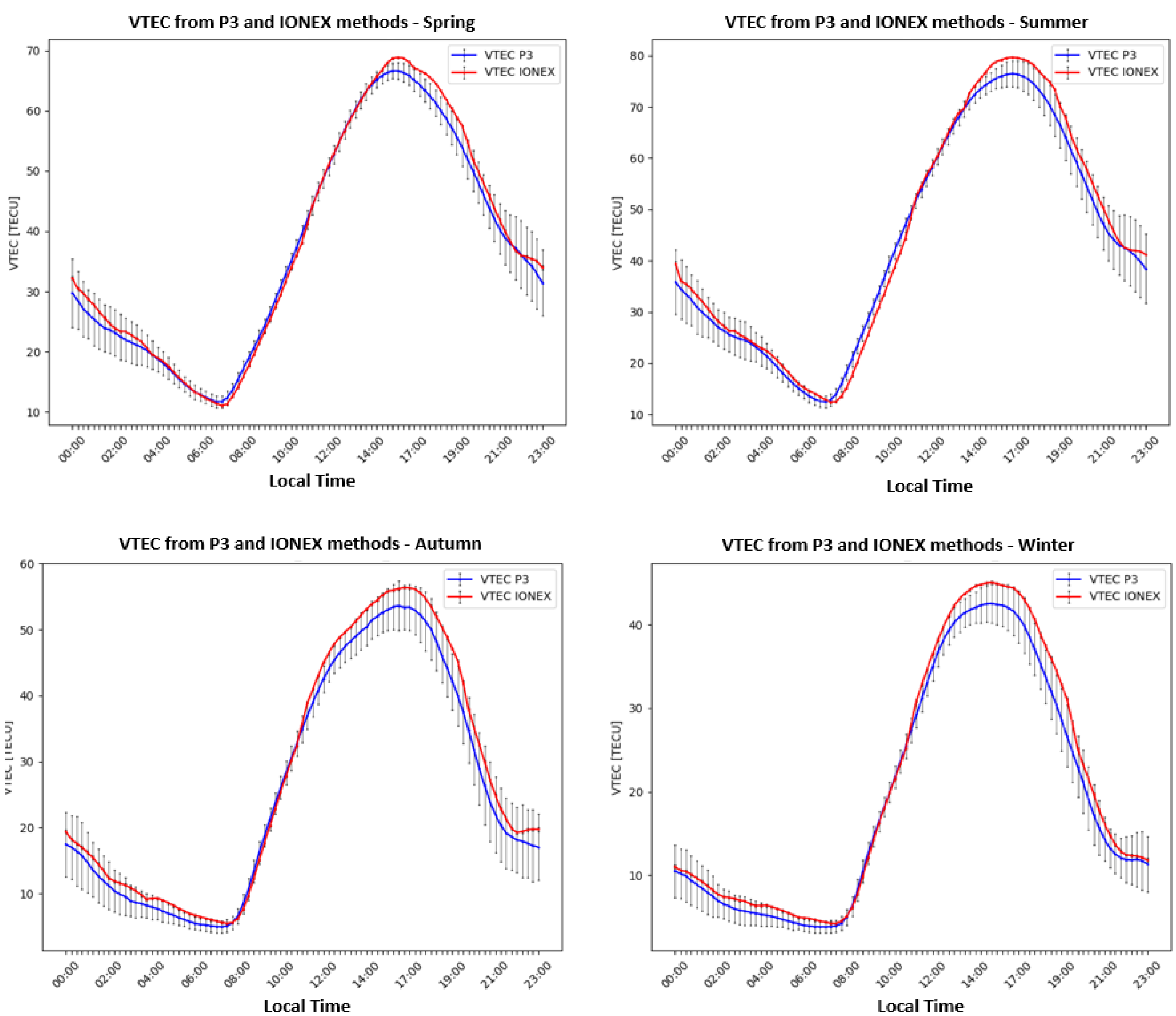

Figure 5 – Comparison between GPS P3 and n ionospheric map methods in Southeast Brazil during seasons (from author).

ANOVA demonstrated no significant statistical difference between the two methods according to the F statistics values calculated for each season. Spring showed the highest convergence with a calculated F equal to 0.008, followed by summer (0.101), winter (0.409), and autumn (0.454).

To observe the behavior of the ionosphere using the GPS P3 method during the geomagnetic storm observed by the BGS magnetometers, the VTEC was calculated between April 21 and 25, 2023, applying the procedure in section 2.4, using the ionvtec_p3_final.py module, from the VtecGraph3 program, as shown in Figure 6 (Yamada, 2024).

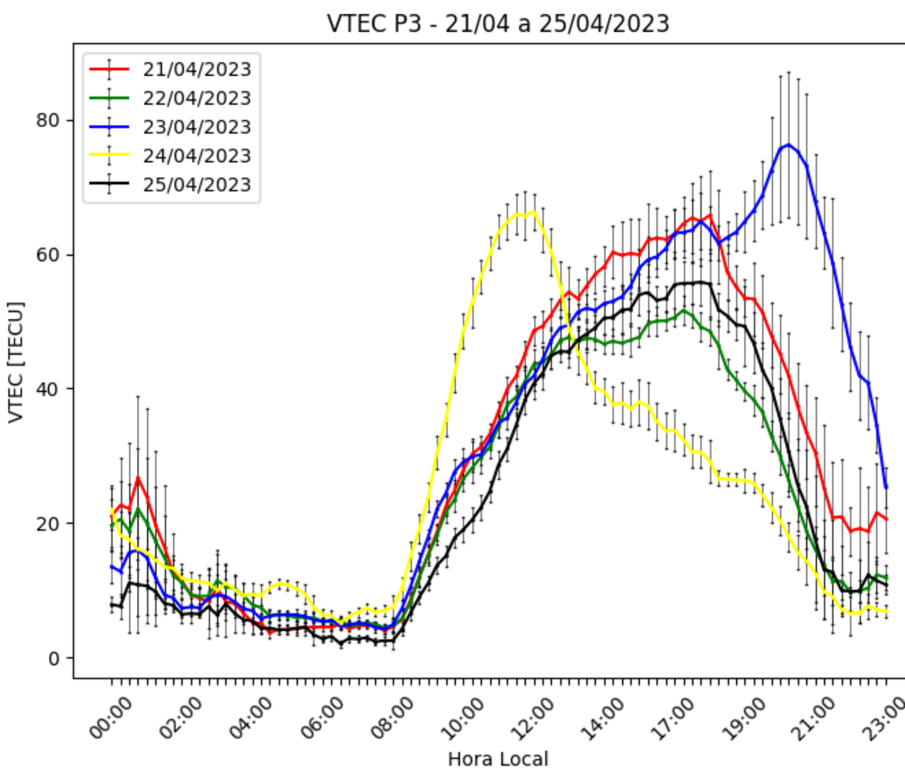

Figure 6 - Behavior of ionosphere in Southeast Brazil during geomagnetic storms in April 2023 (from the author).

Figure 6 highlights the **changes** in the behavior of the ionosphere on the 23rd and 24th of April, 2023. On the 23rd, around 6 pm, even with the beginning of the night period, when normal behavior predicts a decrease in the values of VTEC, an abnormal increase is observed, reaching 76.3 TECU. Then, the curve drops to about 20 TECU around midnight.

On 24/04/2023, behavior considered normal was observed from 0 am until 8 am; from 8 am onwards, the values rose abruptly until reaching the peak value equal to 66.3 TECU at around noon. Then, an abnormal drop in values is observed between 1 pm and 11 pm. On 25/04/2023, behavior returns to normal, showing values below 10 TECU between 0 am and 8 am and a cosine curve between 8 am and 11 pm, with a peak value around 5 pm.

4 Conclusions

Society increasingly depends on services provided by satellite systems. Considering the ionosphere as the most harmful layer of the Earth's atmosphere to the electromagnetic signals emitted by satellites. Research into the behavior of the ionosphere and its effects on electromagnetic signals is becoming increasingly critical. This study showed that it is possible to use a UTC time scale structure to observe the behavior of the ionosphere. The measurements were close to the ionospheric mapping method, widely used to predict and monitor the ionosphere.

It was possible to observe **daily, seasonal, and annual variations in the ionosphere** through measurements of ionospheric delays from the CGGTTS files, recorded by the UTC Time Scale (INXE), located in the district of Xerém, municipality of Duque de Caxias / RJ. It was also possible to observe **changes** in the behavior of the ionosphere **during geomagnetic storms** caused by the solar explosion on April 21, 2023.

Applying a single-layer model mapping function and calculating averages weighted by the receiver distances about sub-ionospheric points made it possible to calculate VTEC values close to those measured and available in the IONEX files of the MAGGIA tool.

The analysis of variance between the two methods, during the year's seasons, in the exact geographic coordinates, demonstrated no statistically significant difference between the values calculated between the two methods.

The characterization of the ionosphere in the southeast region of Brazil during the analyzed period contributes to the scientific community qualitatively and quantitatively. This method can be used in similar laboratory structures. The technical requirements for the ionosphere characterization for laboratories with highly accurate time scales can be achieved with relatively simple structural adaptations. The main investment is acquiring the GNSS signal reception system (geodetic receiver, antenna, and cables) and training the human resources involved.

Furthermore, the characterization of the ionosphere, carried out in this work, can contribute to the development of specific mathematical models for application in single-frequency receivers operating in the southeast region of Brazil to reduce the location errors that mathematical models require.

Acknowledgments

This work was supported by the Brazilian Air Force (FAB) through the Industrial Fostering and Coordination Institute – IFI and the National Institute of Metrology, Standardization, and Industrial Quality – INMETRO through the Scientific-Technical Cooperation Agreement nº 007/ 2020 of July 15, 2020. Special thanks to the Laboratory of Space Meteorology, Terrestrial Atmosphere, Geodesy, Geodynamics, Instrumental and Astrometric Design (MAGGIA) of the

Universidad Nacional de La Plata (UNLP) who provided the IONEX files for comparison with the method developed in this work.

Open Research

The VtecGraph3 program, IONEX, and CGGTTS files used for the characterization of the ionosphere in this study are available at Mendeley Data via Reserved DOI: 10.17632/9vx9nk8bhg.1 (provisional DOI) with Creative Commons Public Domain (CC by 4.0). A provisional link is provided for peer review only: https://data.mendeley.com/preview/9vx9nk8bhg?a=f2b8ea96-ead7-4d7c-9b85-e719c13e9b60 (Anyone with this share link can see your unpublished dataset and will be able to download your files. The link will expire when you publish your dataset or create a new version).

References

BIPM. (2008). JCGM 100:2008 GUM 1995 with minor corrections. Evaluation of measurement data – Guide to the expression of uncertainty in measurement. ISBN 92-67-10188-9. Retrieved from: http://www.bipm.org/utils/common/documents/jcgm/JCGM_100_2008_E.pdf

British Geological Survey. (2022). International Geomagnetic Reference Field (IGRF)**.** Retrieved from: http://www.geomag.bgs.ac.uk/research/modelling/IGRF.html

Dach, R., Hugentobler, U., Fridez, P. & Meindl, M. (2007). *Bernese GPS Software Version 5.0*. Astronomical Institute, University of Bern. Switzerland. Retrieved from: http://ftp.aiub.unibe.ch/BERN50/DOCU/DOCU50.pdf

Feltens, J., Schaer, S., & Gurtner, W. (2015). IONEX: The IONosphere Map EXchange Format Version 1. Darmstadt: [s.n.], update to v1.1. Retrieved from: http://ftp.aiub.unibe.ch/ionex/draft/ionex11.pdf

Frigo, E., & Hartmann, G. (2018). Intensity variation of geomagnetic field in Santa Maria (Brazil) over the past 3 thousand years. *Ciência E Natura*, 40(7). https://doi.org/10.5902/2179460X27696

ITU-T. (2020). *GSTR-GNSS: Considerations on the use of GNSS as a primary time reference in telecommunications*. Retrieved from: https://www.itu.int/dms_pub/itu-t/opb/tut/T-TUT-HOME-2020-PDF-E.pdf

Jaskulski, T., Aveiro, H. C., Moor, L. P., Denardini, C. M., Muralikrishna, P., & Schuch, N. J. (2006). Estudo do plasma ionosférico da anomalia magnética do Atlântico Sul (AMAS) utilizando riômetros. *In:* Congresso regional de iniciação científica e tecnológica em engenharia, 21., 2006, Ijuí. *Annals* [...]. Ijuí: Ed. Unijuí. 2006.

Levine, J. (2016). Coordinated Universal Time and the Leap Second. *The Radio Science Bulletin*. https://doi.org/10.23919/URSIRSB.2016.7909995

Matsuoka, M. T., Camargo, P. De O., & Batista, I. S. (2006). Solar flare impact in the ionosphere and GPS positioning in the Brazilian region: a study case for the October, 28 2003 event.

Bulletin of Geodetic Sciences, 12(2). Retrieved from: https://revistas.ufpr.br/bcg/article/view/7234

Matsuoka, M. T., & Camargo, P. O. (2007). Ionospheric correction using IGS Global TEC Maps: Evaluation at the GPS point positioning in the Brazilian region. *Bulletin of Geodetic Sciences*, Curitiba, 13(2). Retrieved from: https://revistas.ufpr.br/bcg/article/view/10727

Mendoza, L. (2024). Monitoreo a tiempo (casi) real de la ionósfera sobre Sud América. Retrieved from: https://www.maggia.unlp.edu.ar/articulo/2017/1/6/monitoreo_ionosfera

Mendoza, L. P. O., Meza, A. M., & Aragón Paz, J. (2019). M. A Multi-GNSS, Multifrequency, and Near-Real-Time Ionospheric TEC Monitoring System for South America. *Space Weather*, 17(5). https://doi.org/10.1029/2019SW002187

NASA. (2023). What is the Solar Cycle? 2021. Retrieved from: https://spaceplace.nasa.gov/solarcycles/en/

National Oceanic and Atmospheric Administration. (2024). NOAA Forecasts quicker, Strong peak of solar activity. Retrieved from: https://www.swpc.noaa.gov/news/noaa-forecasts-quicker-stronger-peak-solar-activity

NIST/SEMATECH. (2012). *e-Handbook of Statistical Methods*. Retrieved from: https://www.itl.nist.gov/div898/handbook/eda/section3/eda3673.htm. https://doi.org/10.18434/M32189.

Panfilo, G., & Arias, F. (2019). The Coordinated Universal Time (UTC). *Metrologia***,** 56(4). https://doi.org/10.1088/1681-7575/ab1e68

Prol, F. S., Camargo, P. O., & Muella, M. T. D. A. H. (2017). Comparative study of methods for calculating ionospheric points and describing the GNSS signal path. *Bulletin of Geodetic Sciences*, 23(4). https://doi.org/10.1590/S1982-21702017000400044

Riehle, F., Gill, P., Arias, F., & Robertsson, L. (2018). The CIPM list of recommended frequency standard values: guidelines and procedures. *Metrologia*, 55(2). https://doi.org/10.1088/1681-7575/aaa302

Rocha, G. D. C., Marques, H. A., & Galera, J. F. M. (2015). Accuracy of GPS Absolute Positioning with Ionosphere Correction from Global and Regional Ionosphere Maps. *Bulletin of Geodetic Sciences*, 21(3). https://doi.org/10.1590/S1982-21702015000300028

Santos, V. A. (2020). *Uso de dados de redes GNSS ativas para a geração de mapas regionais ionosféricos. 2020.* Master's Thesis – Unesp, Presidente Prudente.

Segantine, P. C. L. (2005). *GPS***:** *Sistema de Posicionamento Global*. São Carlos: USP, 1, ISBN 85-85205-62-8.

Whibberley, P. B., Davis, J. A., & Shemar, S. L. (2011). Local representations of UTC in national laboratories. *Metrologia*, 48(4). https://doi.org/10.1088/0026-1394/48/4/S05

Yamada, F. (2024). “Space Weather - Ionosphere characterization using GPS P3 method by measuring ionospheric delay in Southeast of Brazil and considering geomagnetic storms”, Mendeley Data, V1, https://data.mendeley.com/preview/9vx9nk8bhg?a=f2b8ea96-ead7-4d7c-9b85-e719c13e9b60 (provisional DOI)

Yang, X., Li, J., Zhang, S. (2014). Ionospheric correction for spaceborne single-frequency GPS based on single layer model. *Journal of Earth System Science*, 123(4). https://doi.org/10.1007/s12040-014-0442-z